Liquidus Tracking:

Large scale preservation of encapsulated

3-D cell cultures using a vitrification machine

Eva Puschmann[a*], Clare Selden[a], Steve Butler[b] and Barry Fuller[c]

[a] UCL, Institute for Liver & Digestive Health, Royal Free Campus, London, NW3 2PF, UK
[b] Planer PLC,110 Windmill Road, Sunbury-on-Thames, UK
[c] UCL, Department of Surgery, Royal Free Campus, London, NW3 2PF, U.K.
[*]For correspondence: eva.puschmann.10@ucl.ac.uk

Abstract

Currently, cryo-banking of multicellular structures such as organoids, especially in large volumes at clinical scale >1 litre , ~~and large volumes~~ remains elusive for reasons such as insufficient dehydration and cryoprotectant additive (CPA[1]) penetration, slow cooling and warming rates and devitrification processes. Here we introduce the concept of Liquidus Tracking (LT) using a semi-automated device for liquid volumes of up to 450ml including 130ml of alginate encapsulated liver cells (AELC) that archived controlled and reversible vitrification with minimized toxicity.

First a CPA solution with optimal properties for LT was developed by employing different small scale test systems. Combining sugars such as glucose and raffinose with Me_2SO improved post-exposure (at +0.5˚C) viabilities from 6 +/- 3.6% for Me_2SO alone up to 58 +/- 6.1% and 65+/-14.2 % respectively ($p<0.01$). Other permeating CPAs (e.g. ethylene glycol, propylene glycol, methanol) were investigated as partial replacements for Me_2SO. A mixture

[1] cryoprotectant additive (CPA), Liquidus Tracking (LT), alginate encapsulated liver cells (AELC), alpha-fetoprotein (AFP), mixture of Me_2SO, ethylene glycol and glucose (ratio 4:2:1): termed LTdeg.

of Me_2SO, ethylene glycol and glucose (ratio 4:2:1– termed LTdeg) supported glass-forming tendencies with appropriate low viscosities and toxicities required for LT. When running the full LT process, using Me_2SO alone, no viable cells were recovered; using LTdeg, viable recoveries were improved to 40+/-8% ($p<0.001\%$). Further refinements of improved mixing technique further improved recovery after LT. Recoveries of specific liver cell functions such as synthesis of albumin and alpha-fetoprotein (AFP) were retained in post thaw cultures. In summary: By developing a low-toxicity CPA solution of low viscosity (LTdeg) suitable for LT and by improving the stirring system, post-warming viability of AELC of up to 90% and a AFP secretion of 89% were reached. Results show that it may be possible to develop LT as a suitable cryogenic preservation process for different cell therapy products at large scale.

Keywords

Liquidus Tracking, large volume vitrification, CPA toxicity, Bioartificial liver device

Introduction

Scientists have successfully cryopreserved a variety of cells over the last 40 years, but success has mainly been achieved by traditional slow cooling with cell suspensions in small (<10 ml) volumes [16,45] in tube format, or in bag format in volumes of up to 200ml [10,17,33]. Cooling multicellular systems down to deep sub-zero temperatures has proven far more challenging, especially when large volumes of biomass require cryo-banking. These problems began to be understood during early attempts to cryopreserve whole organs or large complex tissues. They were mainly related to the formation of extracellular ice in liquid spaces within the tissue [37], such as within small capillary blood vessels inside an organ [19], which physically destroyed the internal structure. In addition, disruptive ice propagation between inter-connected cells [1], insufficient cell dehydration and CPA penetration during slow cooling and ice-recrystallization during the warming process have all been noted. These can

also make cell agglomerates more susceptible to freezing damage than individual cells. Ice formation can be avoided by vitrification, but high cooling rates must frequently be imposed to avoid toxic effects from the essentially high CPA concentrations required and to maximise the likelihood of achieving the glassy state without ice nucleation events [13]. This remains a significant challenge for large tissues or, equally, for large volumes of functionally interconnected cells such as cell spheroids, as enough time must be given for CPA to penetrate into the all the cells, including those in the core, and for the core cells to dehydrate sufficiently to avoid intracellular freezing, risking toxic effects during CPA exposure and cooling. CPA toxicity is also critical during the warming process when high concentrations of CPAs will be present when the cryogenic glasses begin to liquefy; equally the high warming rates needed to prevent devitrification and ice re-crystallisation for all cells within a sample are difficult to achieve in large volumes [6,7].

Many of those obstacles can be overcome by Liquidus Tracking (LT), a method of achieving vitrification in an aqueous mixture by incrementally increasing concentrations of penetrating CPAs (up to 70%) at incrementally decreasing temperatures [15,38,47]. Cryoprotectants are known to be less toxic at lower concentrations, but also at lower temperatures [34,48] due to decreased cell activity, reduced chemical interaction with sensitive biomolecules and reduced CPA permeation. Due to reduced CPA toxicity, and avoidance of ice nucleation in LT, large samples can be vitrified without the necessity of fast cooling rates, or when longer exposure times are required to allow for sufficient CPA penetration - for example for organ and tissue vitrification.

We have previously studied cryopreservation by slow cooling of alginate encapsulated multicellular liver cell spheroids (AELC) in developing a bioartifical liver support system [31]. Treatment volumes of between 1-2 litres of AELC for use in a bioartificial liver device have been used in our pre-clinical studies [11] and are predicted to be needed for patient

therapy. We have also shown that LT vitrification can be applied to AELC in a small volume feasibility study [40]. Our aim here was to develop a LT protocol, which would allow the cryo-banking and warming of large volumes of AELC whilst maintaining good functional recovery. To improve cell viability we have developed a low-toxicity CPA solution for LT with the requirement of low viscosity (but which – nevertheless – could suppress ice nucleation) so that it may be used within the Liquidus Tracker equipment. Additionally the development of a new stirring system substantially increased post-warming viability.

Materials and Methods

Unless otherwise stated, all chemicals were sourced from Sigma (Poole, United Kingdom) and for cooling and warming a PlanerLiquidus Tracker Controller and a Controlled Rate Freezer (Planer, Kryo 10, Series II chamber) was used. CPA concentrations were used and reported in weight per volume (w/v) throughout this work.

Cell culture and encapsulation

The techniques for culturing HepG2 cells and producing AELC have been described previously in detail [11]. In brief: Confluent HepG2 monolayer cells (from ECACC, Wiltshire, UK) were encapsulated into 1% alginate (alginic acid sodium salt *Macrocystis pyrifera* kelp) by calcium-related polymerisation and cultured for >11 days until containing several thousand cells in spheroids within each alginate bead (average diameter 450µm).

Cell culture to different end cell densities

For experiments that required different cell densities, AELC were cultured for either 3, 5, 7, 9 or 11 days before being used for LT.

Viability assay

Cell viability was measured by dual staining with fluorescein diacetate and propidium iodide using an established imaging software method for quantification which has been established

against cell number and protein production [21]. Viability was measured after 24 hours post-treatment, the time point of lowest viability before on-set of recovery [31].

Quantification of cell numbers

Cell number quantification using the Nucleoview System (Sartorius Stedim, Epsom, United Kingdom) has been described previously in detail [11]. Viable cell numbers were calculated by multiplying the cell number by the viability for each sample.

Functional assays to assess protein synthesis by alpha-fetoprotein and albumin secretion

Alpha-fetoprotein (AFP) and albumin synthesis and secretion were measured by sandwich enzyme-linked immunosorbent assay which has been described previously in detail [11].

Viscosity assessment and measurement

Viscosity of CPA mixtures is an important factor in applying LT to facilitate good mixing and ensure uniform high CPA concentrations to avoid ice nucleation. Viscosity of CPA solutions was assessed for applicability by comparing new CPA solutions against a reference solution (70% (w/v) Me_2SO) by observational grading of resistance to pipetting or to manually stirring the solution at -40˚C – the lowest workable LT temperature from previous experience [40]. For pipetting a standard 1ml Eppendorf pipette and 1ml pipette tips and for stirring a stainless steel spatula with a 4mm width were used. 10ml CPA in 15ml Centrifuge tubes (Falcon, Fisher Scientific) were cooled to -40˚C. This test was developed as no viscometers or rheometers operable at -40˚C were available locally and it also allowed direct rapid assessment of multiple samples. Viscosity was rated 1-4 (1 = similar to 70% (w/v) Me_2SO, easy to pipette; 2 = pipetting not possible but can be easily stirred, 3 = very viscous, stirring very difficult, 4 = stirring not possible, almost a solid). Solutions with a viscosity rating of "2" were modified by replacing 10% of the highly viscous CPAs with less viscous CPAs. In particular methanol was selected as a low viscosity CPA to reduce the overall viscosity of the mixture. Thereafter, viscosities of the most promising CPA solutions were

measured at 20˚C using a Bohlin CVO automated shear rheometer to provide a set of reference data. Shear stress (s^{-1}) was increased by 10rpm every 10 seconds, from 10 to 250rpm.

CPA toxicity tests

A two-step protocol was used to reduce potential CPA-related osmotic injury based on previous experience with AELC which have shown high viabilities after one step addition and dilution of up to 40% Me_2SO (v/v) [40]. A volume of 0.25ml settled beads (AELC) was incubated in a 30% (w/v) CPA solution for five minutes at room temperature (Falcon tubes, Fisher Scientific), then for five minutes at 0.5˚C (tubes in ice-water). The concentration was then increased to 60% (w/v) CPA and beads incubated for 10 or 20 minutes at 0.5˚C. CPA concentration and incubation time were chosen to display strong difference in survival between solutions. By adding 1xPBS for dilution steps, the CPA concentration was reduced to 30% (w/v). Samples were left on ice for five minutes. Beads were washed twice with 4ml of 1xPBS and incubated in complete medium for 24 hours before viability was assessed.

Optical vitrification assessment

A volume of 4ml of each newly developed CPA solution and Me_2SO at a concentration of 60% and 70% (w/v) was vitrified in a 12-well plate by cooling samples at -10℃/min to -160℃. All solutions were then left at room temperature for warming and optical observation.

Standard small volume vitrification protocol

A traditional two-step small volume protocol was used to assess vitrification of AELC *per se* and allow comparison to LT. Therefore 0.25ml settled beads were incubated in a 31.5% (w/v) CPA solution in Nunc cryo-tubes (1.8 ml, Nunc, Loughborough, UK), first for five minutes at room temperature and then for an additional five minutes at 0.5˚C (tubes in ice-water). The CPA concentration was increased to 63% (w/v) using a 70% (w/v) pre-cooled CPA solution (at 0.5˚C). Samples were left on ice for five minutes and then plunged into liquid nitrogen.

147 Samples were warmed for approximately eight minutes on ice until they reached a liquid
148 state. By adding ice cold 1xPBS (+Mg^{2+}, Ca^{2+}) the CPA concentration was reduced to 31.5%
149 (w/v). Samples were left on ice for five minutes before washing twice with 4ml 1xPBS
150 (+Mg^{2+}, Ca^{2+}). Finally, AELC were incubated in complete media for 24 hours before
151 assessing viability.

152 **Liquidus Tracking**

153 The prototype Planer LT machine consists of a sample carrier with a magnetic stirrer which is
154 placed inside a Controlled Rate Freezer (Planer, Kryo 10, Series II chamber) and an inlet and
155 outlet pump system [40]. All of these units are connected to a controller, which allows a
156 completly automated cooling, mixing and addition and extraction process when using a single
157 highly concentrated CPA solution. For the work presented here the peristaltic pumps were
158 operated manually to allow for the use of differently concentrated CPA inlet solutions for
159 both the cooling and warming process. A liquid volume of 450ml including 130ml of settled
160 beads was used for each run, if not stated otherwise.

161 **(i)** LT cooling: The controlled rate freezer was first set on hold at -20˚C and then -25˚C until
162 the sample reached a concentration of 32% (w/v) at -12˚C and 40% (w/v) at -16˚C,
163 respectively, by pumping in a 50% CPA inlet solution. After that the freezer was set to -
164 30˚C and a 60% (w/v) CPA solution was used to increase the sample to 50% (w/v) (at -
165 20˚C) and subsequently a 66% (w/v) CPA solution was added to reach a final sample
166 concentration of 64% (w/v) (at -20˚C). CPA increase to 25% (w/v) were carried out by
167 addition only, increase to 64% (w/v) was reached by operating both inlet and outlet
168 pump simultaneously at a flow rate of 20ml/min. Then the freezer was set to -160˚C to
169 cool the sample below the predicted glass transition temperature of about -121˚C.
170 Samples were held for a minimum of 10 minutes below -125˚C (Figure 2). The
171 temperature was measured in the middle of the sample carrier, where cooling is slowest.

(ii) LT warming: The sample carrier remained inside the freezer but with the liquid nitrogen supply shut off for slow warming to -95˚C. For fast warming to -40˚C the sample carrier was placed outside the freezer at room temperature. For LT reversed warming, first 500ml of a 50%, then a 40% and then a 30% (w/v) CPA solution were pumped in at 20ml/min to decrease the sample CPA concentration. Simultaneously sample solution was extracted at 20ml/min. The freezer holding temperature was increased from initially -25˚C to -20˚C and then -15˚C for 30 minutes. Finally, the freezer was set to -10˚C and 1L 1xPBS (at 20˚C) was added to decrease the sample CPA concentration to 0% (Figure 2).

The temperature-concentration curve

For each LT run the temperature/concentration (T/C) curve was determined by measuring the CPA concentration of the chamber outlet solution and by correlating this value to the sample temperature reached at the end of the extraction cycle. Thermocouples inserted into the inlet and outlet tube and inside the sample carrier were used to monitor the temperature. The refractive index (Digital Refractometer, Cole-Pamer Brix, 45.0 to 95.0%, EW-02941-33) was used to determine the CPA concentration of the outlet solution based on a previously established standard curve [40].

Filter system

To maintain AELC beads (average diameter (d) =450μm) inside the sample carrier during CPA extraction and to avoid filter blockage, a plastic tube (5cm length, d=4cm) was covered from both ends with a 100μm mesh through which the outlet port was introduced. The filter was placed 1cm away from the opening of the port – where the suction force was highest – to avoid the filter getting blocked by beads.

Avoiding devitrification

To ensure that devitrification during warming was avoided, a finally sample CPA concentration of 64% (w/v) had to be reached, before the fast cooling process to below -121˚C was started.

Differential scanning calorimetry

To establish the liquidus curve of the newly developed CPA solution, differential scanning calorimetry (DSC) was used to determine the equilibrium melting point of increasing CPA concentrations. The method has been described previously in detail [32].

Statistics

Statistical analyses were performed by Student's *t*-Test using Excel software.

Results

CPA development

(i) Viscosity - candidate CPA combinations

It was predicted that at least 40% (w/v) penetrating CPAs and a maximum total concentration of 70% (w/v) CPA should be used to obtain sufficient vitrification for large volumes and slow cooling rates (<10˚C/min) from previous feasibility studies [40]. By using the observational viscosity test at -40˚C only four solutions were identified with a similar viscosity to 70% (w/v) Me_2SO when comparing (in increments of 10%) combinations of Me_2SO, EG and PG with the non-penetrating CPA glucose. All of these solutions contained at least 40% (w/v) Me_2SO, but only 10% (w/v) glucose. The viscosity of another eight solutions was sufficiently reduced for Liquidus Tracking through the substitution of 10% (w/v) of a penetrating CPA with methanol (Figure 1). Viscosity of CPA solutions of lowest toxicity were additionally measured with a Bohlin® CVO automated shear rheometer at 20˚C displaying lowest viscosity for 70% (w/v) Me_2SO with 4.62mPa·s and highest viscosity for 40% Me_2SO with 20% EG and 10% glucose (w/v) with 6.51mPa·s (Table 1).

(ii) Testing different sugars and sugar combinations

To improve post-warming LT cell survival, non-penetrating sugars were added to Me_2SO, which yielded poor AELC viability when used as a single CPA. Viability of AELC, incubated in 50% (w/v) Me_2SO, decreased from 90% +/- 2.15 (n=5) to 5.9% +/-3.6 (n=5). The addition of 10% (w/v) of any sugar (glucose, fructose, raffinose, sucrose, trehalose) increased cell viability markedly by up to 50% although the final CPA concentration was increased to 60% (w/v). The combination of glucose with another sugar (5% (w/v) each) did not significantly increase cell viability (Figure 3).

(iii) Toxicities of low viscous CPA solutions

Glucose was chosen as a CPA additive because it is readily available in large quantities, inexpensive and is clinically used. In a pre-screening toxicity test, solutions containing methanol (10% w/v) were generally more toxic to AELC than those without. Methanol was only well tolerated when the Me_2SO concentration was equal or less than 30% (w/v) and with at least 10% (w/v) EG. The toxicity test was repeated in more replicates with the five most promising solutions. Additionally, these solutions were used to vitrify AELC in a standard small volume approach (Table 1, Figure 1). Both tests revealed the same order of performance with highest viability after treatment being obtained with Me_2SO/EG/glucose at a ratio of 4:2:1, followed by a combination of Me_2SO/EG/methanol/glucose at a ratio of 2:3:1:1 (Table 1). EG exhibited lower toxicity to AELC than Me_2SO and PG when in combination with Me_2SO. However, a solution of only EG and glucose (6:1), defined too viscous for LT (data not included in Table 1), exhibited significantly higher toxicity to AELC than the combination of EG, glucose and Me_2SO with 50% versus 68% remaining viability ($n=5$, $p<0.01$).

(iv) Vitrification properties of low toxic CPA solutions

All five low toxicity solutions (Table 1 – solutions >90% viability (test 1)) vitrified (visual avoidance of ice formation) at a concentration of 70% (w/v), but only Me_2SO and a combination of Me_2SO/EG/Glucose in a ratio 5:1:1 vitrified (visual absence of ice) at 60% (w/v) (Figure 1). Those solutions that did not vitrify at 60% (w/v) contained 20% (w/v) or more EG. It was observed that ice disappearance during warming was slowest for a solution with Me_2SO/EG/Glucose in a ratio of 4:2:1 (LTdeg), which was the only one that did not contain 10% (w/v) methanol. Increasing the overall CPA concentration proportionately to 64% (w/v) was found to be consistent with avoidance of visible ice during warming with LTdeg.

Standard small volume vitrification experiments were performed using the 5 CPA solutions of lowest toxicity and compared with the outcomes for toxicity testing without cryo-cooling at 0.5˚C. Recoveries of viability after 24h culture for vitrification experiments post thaw were very low using Me_2SO alone (around 1%), whilst the best outcomes (53%) were seen with LTdeg (Table 1, Figure 1). From these range setting experiments, LTdeg was chosen to take forward into the full LT investigations.

Liquidus Tracking experiments

(i) Heat transfer measurements

When the first LT runs were carried out, using Me_2SO as a cryoprotectant, (with a freezer cooling rate of -1˚C/minute and a liquid volume of 450ml), the temperature of the sample inside the sample carrier was approximately 20˚C higher than the temperature of the Me_2SO equilibrium melting point and 15˚C higher than the predicted target temperature. To increase the sample cooling rate by improving heat transfer, the freezer temperature was set up to 10˚C below the predicted Me_2SO liquidus curve. Although the CPA concentration inside the outlet tube and the sample carrier is comparable, the solution inside the insulated outlet tube

froze at sub-zero temperatures, as a result of its geometry and the resulting higher cooling rate. To avoid this, first infusions were carried out by operating the pumps manually, and the outlet was primed with 50% (w/v) CPA when not in use. This allowed the freezer temperature to be set on hold at -20˚C and to maintain the sample/concentration curve close to the liquids curve until a concentration of 25% (w/v) CPA at -8˚C was reached, before using inlet and outlet pump simultaneously (Figure 4).

(ii) Machine delivered LT: Me_2SO alone vs. new CPA solution

Initial LT runs using the pump-driven mixing with a volume of 450ml (including 130ml of settled beads) using Me_2SO as a single CPA resulted in no post-warming cell viability. When the newly developed CPA solution Me_2SO/EG/Glucose (4:2:1) was used, cell viability was increased to 40% (+/- 7.7%) (n=3).

(iii) Inhomogeneous "cell per bead" survival

It was noted in preliminary studies by using fluorescence microscopy that some of the beads contained a high proportion of viable cells, while others contained almost exclusively dead cells after re-warming from LT. It was assumed that the effect was caused by the temperature difference within the sample carrier (e.g. colder at the carrier wall, bottom or surface and warmer at the centre). Viability up to a CPA concentration of 35-40% (w/v), reached at a temperature of -15˚C, remained high and inhomogeneous AELC viability in beads was not observed. The inlet temperature was therefore maintained at -15˚C, while increasing the CPA concentration from 35 to 64% (w/v), to avoid any potential CPA toxicity effects related to temperature differences within the system. Nevertheless, strong variations in viabilities between individual beads were observed. It was suspected that stirring the entire sample volume was inefficient, resulting in regions of poor CPA mixing and therefore potential ice nucleation.

(iv) The Liquidus Tracking stirrer

To achieve more homogenous mixing conditions, the original Planer stirrer, designed to hold larger tissue constructs in the middle of the sample carrier while providing efficient CPA homogenisation, was replaced with a simple propeller stirrer. By using the new propeller stirrer, viabilities post LT were significantly improved from 38% +/-11.7 to 77% +/- 4.3 (n=4 +/-SD) and strong variations in viable cell numbers between different individual beads were no longer observed (Figure 5).

(v) Cell density impacts cell survival

Alginate encapsulated spheroids (AES) of high cell densities ($15x10^6$ cells/ml of beads) were less affected by LT treatment with new stirrer than AES of low cell density ($4x10^6$ cells per ml/beads) with viabilities of 57% +/-9.7 and 11% +/- 6.9, respectively ($n=17$, $p<0.01$). Both cultures were processed within the same run. Beads of either type were easily distinguished under the microscope, which made it possible to take images of single beads and determine the viability using the established FDA/PI method.

Although this procedure allowed testing of two populations of beads under exactly the same conditions, cell number and protein synthesis could not be determined because beads of different cell densities could not be physically separated. Thus, single run experiments were carried out with batches of either high or low cell density beads. Again higher cell density resulted in higher cell numbers, viability, albumin and alpha-fetoprotein production post LT cooling with respect to the positive control. For cell densities of $17x10^6$ and $20x10^6$ cells/ml of beads viability was 70% and 90%, viable cell numbers were 67% and 96% and albumin and alpha-fetoprotein release were 48% and 57%, and 80% and 88%, respectively (fraction of the untreated control after 48 hours of post warming – Figure 6).

Discussion

Choice of CPA for LT

We observed here that the pumps and stirrer of the semi-automated Liquidus Tracker are impaired above a viscosity of approximately 900 mPa·s (Me_2SO at -40˚C). Thus, viscosity was identified as the first limiting factor for developing a new LT CPA solution. Dimethyl sulfoxide (Me_2SO), ethylene glycol (EG) and propylene glycol (PG) were selected as penetrating CPAs based on their relatively low viscosity and their common use in vitrification protocols. Only four combinations (in increments of 10%) of Me_2SO, EG and PG with 10% (w/v) glucose were of sufficiently low viscosity for our purpose. For this reason, viscosity was reduced by replacing 10% of a higher viscous penetrating CPA with methanol.

Monovalent alcohols are not commonly used in cryopreservation protocols, mostly due to their known high toxic effects on many biological systems. However, methanol has been used successfully in fish semen and embryo preservation [24,25,42]. In these applications, the concentration used was 10% or less, which justified the concentration used here. Although of general high toxicity, methanol was well tolerated when combined with EG and low amounts (<=30% w/v) of Me_2SO and due to its high permeability [5] might be considered useful for some vitrification protocols.

Sugars are generally used to decrease the amount of penetrating CPAs while keeping similar final CPA concentrations and glass-forming tendencies. When testing different sugars for our LT CPA solutions, Me_2SO was not replaced, but instead 10% (w/v) sugar was additionally included. The type of sugar used in our studies appeared to be irrelevant, which might suggest a general effect like reduced osmotic stress. It is known that sugars osmotically reduced the cell volume, and therefore triggering reduced uptake of penetrating CPA, which leads to less intracellular dehydration through CPAs and also reduced osmotic stress when

339 CPAs are washed out. However, we have previously shown that AELC maintain high
340 viability after one-step addition and dilution of up to 40% (v/v) Me_2SO when carried out at
341 low temperatures [40]. The fact that AELC can support strong osmotic changes and that
342 toxicity is generally and strongly decreased at low temperatures (osmotic stress has been
343 suggested to increase at lower temperatures as the difference between transmembrane water
344 fluxes and movement of penetrating CPA increases [2]) might also indicate additional
345 effects, such as cell membrane stabilization or even some sort of biochemical toxicity
346 neutralisation comparable to that reported for reduced toxicity of formamide through the
347 addition of Me_2SO [12]. For the semi-automated LT process osmotic stress is even further
348 reduces as lower concentrated CPA solution is continuously added while being mixed by a
349 stirrer. However, further work will be needed to assess the relevant importance of osmotic or
350 chemical toxicities within the overall context of LT.

351 Glucose was chosen for further LT studies for two reasons; firstly because it is clinically
352 available and inexpensive and for automated LT large CPA volumes are needed and secondly
353 because glucose has been reported to prevent irreversible binding of Me_2SO to proteins [8].

354 EG is stated to be the least toxic CPA for hepatocyte virtification [23,30] but for AELC in
355 LT, the combination of Me_2SO (40% w/v) and EG (20% w/v) with 10% (w/v) glucose,
356 resulted in significantly higher viability than either of the CPAs on its own with 10% (w/v)
357 glucose. This observation corresponds to previous findings from other authors in
358 chondrocytes and alginate encapsulated HepG2 and β-TC-cells, which suggest that
359 combinations of penetrating CPAs are less toxic than the use of a single CPA [20,26,46]. We
360 could find no explanation for the interaction between EG and Me_2SO, but both solutions are
361 also main components of the well-known and commercially available vitrification solutions
362 VS55 and M22 [12,14]. A similar composition of 22% EG and 18% Me_2SO and 17.5% for

363 both EG and Me_2SO have also shown good results for the vitrification of cumulus cells [41]
364 and equine embryos, respectively [35]. It is interesting, that – although developed to be first
365 of low viscosity and second of low toxicity – our final chosen LT solution for AELC
366 resembled those that are already commercially sold for other standard vitrification protocols.
367 We speculate that viscosity plays an important role in realizing an optimum between CPA
368 penetration and dehydration.

369 When developing new CPA mixtures, it is necessary to assess toxicity of cryoprotectants at
370 the concentrations needed to vitrify. To get an estimation of the vitrification properties of the
371 potential CPA solutions, Me_2SO and the five CPA solutions of lowest toxicity to AELC were
372 vitrified in small volumes and CPA solutions (without AELC) and were optically compared
373 for ice formation. Optical assessment of vitrification is only a semi-quantitative method
374 compared to other physical measurements such as DSC, but it has been used in other studies
375 [18,50]as a direct method which can allow multiple conditions to be investigated at the same
376 time. Whilst all solutions vitrified at 70% (w/v) CPA, only Me_2SO and the mixture of
377 Me_2SO/EG/glucose with a ratio of 5:1:1 vitrified at 60% (w/v) final CPA. One probable
378 explanation why the other four solutions did not vitrify is the higher concentration of EG and
379 methanol. EG has been described as a less effective vitrifier than Me_2SO and PG [3] and
380 methanol only vitrifies on its own under high pressure [6]. However, methanol seemed to
381 have increased the rate at which ice melts during the warming phase, which could be
382 advantageous for decreasing the amount of potential devitrification.

383 The top five low toxicity CPA solutions used to manually vitrify AELC in small volumes
384 performed generally in the same order as they did in the toxicity studies. Reduced incubation
385 time before plunging AELC into liquid nitrogen could be beneficial for solutions with higher
386 concentrations of fast penetrating CPAs (Me_2SO, methanol), and some solutions might vitrify

at lower concentrations which would reduce CPA toxicity and increase viability. For the chosen set-up the solution of lowest toxicity was superior to the other solutions and proved to be an efficient vitrifier in the small volume protocol.

Final CPA concentrations for LT are of less risk for toxicity than for conventional vitrification, as they are reached at very low temperatures (<-30˚C), at which CPA penetration and toxicity are suspected to be strongly reduced. However, at higher temperatures CPA toxicity is to be crucial for cell survival during the LT process. This would point to choosing the lowest toxicity CPA mixture instead of the best vitrifier for AELC preservation by LT.

The ~~semi-automated~~ machine-delivered LT process

Although LT allows for much slower cooling rates than conventional vitrification, cooling rates can be still too slow in respect of practicality when large volumes are being cooled. In our system heat is transferred in two ways: conduction and convection. As the inlet is led through a tube of several meters that is kept within the freezer chamber, the temperature of the inlet solution was found to match that of the freezer chamber at the moment of addition. The shape of the LT sample carrier (small surface area to volume ratio) is unfavourable for fast cooling and warming rates by conduction. When the temperature difference between the freezer chamber and sample is small, both conduction and convection have consequently little impact on the overall sample temperature. Moreover, first CPA addition steps only require small amounts of highly concentrated CPA solution to increase the sample concentration. Thus, the initial temperature change by convection can be neglected. For our work, neither sample volume nor the geometry of the sample carrier could be changed. However reducing the freezer temperature from 5˚C above to 20˚C below the predicted liquidus curve helped to increase the sample cooling rate, although the risk of outlet tube

freezing had to be resolved. Using more inlet volume of lower concentrated CPA, thus increasing convection, can further be used to increase the cooling rate but is logistically more challenging. This type of approach for LT could be described as semi-automatic; the pumps had to be operated by manual control to balance the relative volume exchanges as described; however, the pumps allowed better overall control of solution movement than could be achieved for example by manual decanting.

No viability of AELC was detected when Me_2SO was used for semi-automated LT, but was increased to approximately 40% viability when Me_2SO was replaced with the newly developed CPA solution, suggesting that CPA toxicity and/or osmotic injury was not fully suppressed by the LT process. Inhomogeneous distribution of viable and dead cells between alginate beads led to the assumption that temperature differences within the LT system had caused this effect. The inlet temperature during the cooling process is much colder than the sample temperature and there is also a temperature gradient across the sample carrier with lower temperatures at the outside and higher temperatures on the inside of the sample container. Inhomogeneous distribution of viable and dead cells was not noted for CPA concentrations below 35% (w/v), normally reached at -15˚C. Consequently, the inlet and sample solution temperature were maintained at -15˚C, thus offsetting the temperature difference inside the sample carrier, while the sample CPA concentration was increased to 64% (w/v). However, strong variations in the number of viable cells per bead were still detected, excluding temperature as the main factor for CPA toxicity.

Another possibility was that the method of stirring was the cause of this effect. The original Planer stirrer was designed to operate alongside the sample carrier wall to avoid any interference with larger, static constructs in the middle of the sample carrier. However, this design exhibits strong differences across the sample carrier in respect to mixing behaviour.

For example, AELC trapped between the static pedals and the moving part of the stirrer are subject to stronger mixing and higher shear forces than AELC that are located at the centre of sample carrier. To overcome these mixing differences a propeller stirrer was designed. As a result viabilities were increased to around 80% and viable and non-viable cells were evenly distributed across alginate beads. The inlet port being in close proximity to the Planer stirring system is consistent with the theory that AELC located in the "intense mixing zone" and close to the inlet of highly concentrated CPA, experienced high intra- and extracellular CPA concentration differences and an enhanced mass transport across membranes as a result of high kinetic energy caused by intensive stirring. Thus, chemical toxicity [12], dehydration and osmotic stress [44] may have been reinforced through vicious mixing with this system, which were improved by use of the propeller stirrer.

An interesting effect was seen when beads of varying cell densities were used for LT. Low cell density beads tested in the same experiment, and therefore undergoing exactly the same procedure as did high cell density beads, showed significantly reduced cell survival post recovery. To measure cell numbers and protein release exclusively, experiments with beads of the two different cell densities had to be independently repeated, but the outcomes were the same. 3D cell cultures of higher cell density showed higher post-warming viability, cell number and protein release. This is in accordance with previous observations: Higher cell recovery of hepatocyte spheroids in comparison to single cell suspension following cryopreservation has been reported by Lee and colleagues [27] and vitrification studies with primary rat hepatocytes by Magalhães have shown better post-cryopreservation viability for tissue-like culture than for single cells. They concluded that cell-to-cell contact is beneficial in the maintenance of viability [29]. This might be due to higher cell activity in 3-D cell cultures [37, 38], which has been linked to higher cell recovery following cryopreservation in

459 single cell suspension [7]. It should be pointed out that the BAL system would require high
460 cell density (i.e. high total cell numbers) beads for clinical application [43].

461 In respect of shear forces created by the stirrer during LT, it can be expected that higher cell
462 density is beneficial, as the outer cells may provide protection to those located closer to the
463 centre. This also applies in respect of excessive dehydration. In 3-dimensional cell constructs,
464 water diffuses sequentially from one cell to its neighbour. Cells in the surface layer respond
465 to osmotic changes in the extracellular medium; interior cells respond only to osmotic
466 changes in cells of surfaces, and thus are exposed to slower rates of dehydration [28]. Shear
467 stress is also likely to cause cell death by membrane disruption [36] and would account for a
468 more homogenous distribution of viable and dead cells amongst beads when the propeller
469 stirrer was used. However, with the current LT set up, shear stress would not seem to be a
470 major injurious factor.

471 To further improve the LT system, it would be highly advantageous if the intracellular CPA
472 and water concentration over the LT process could be monitored. For example, if it can be
473 shown that CPA toxicity is negligible once CPA and water flux are (nearly) reversed and in
474 the case that this happens within the temperatures range (0 to -40˚C) of CPA addition and
475 reduction, LT protocols could be suitably adapted. The CPA concentration could then be
476 increased at a higher temperature to ensure intracellular vitrification before cooling the
477 sample. Once reached, the concentration needed to prevent devitrification during warming
478 could be manipulated, for example, by using ice blocking agents [49] to minimise the risk of
479 unwanted ice nucleation.

480 **Conclusion**

481 This work has shown that it is possible to use LT to vitrify large volumes of cell therapies
482 such as AELC in the 3-D format. Further improvements to equipment technology, especially

in respect to more automatization are required. An optimized stirring and CPA inlet system, as well as the use of 3D cultures of higher cell density (>20x10^6 cells/ml beads) may further increase post-warming viability and performance in the future. In theory, the LT volume could be further up-scaled by engineering a larger cell chamber with a scaled stirrer system.

Acknowledgement

We also thank Dr. Paul Matejtschuk and Kiran Malik (NIBSC, a Centre of the Health Protection Agency) for enabling DSC analysis.

Funding

We thank Planer Plc, the Liver Group Charity and the Welcome Trust for funding this study.

References

[1] J.P. Acker, L.E. McGann, The role of cell-cell contact on intracellular ice formation, 1989. 19 (1989) 367–374.

[2] Y. Agca, J. Liu, J.J. McGrath, a T. Peter, E.S. Critser, J.K. Critser, Membrane permeability characteristics of metaphase II mouse oocytes at various temperatures in the presence of Me2SO., Cryobiology. 36 (1998) 287–300.

[3] A. Baudot, L. Alger, P. Boutron, Glass-forming tendency in the system water-dimethyl sulfoxide, Cryobiology. 40 (2000) 151–158.

[4] M. Bokhari, R.J. Carnachan, N.R. Cameron, S.A. Przyborski, Culture of HepG2 liver cells on three dimensional polystyrene scaffolds enhances cell structure and function during toxicological challenge, J. Anat. 211 (2007) 567–576.

[5] J.J. Brand, K.R. Diller, Application and theory of algal cryopreservation, Nov. Hedwigia. 79 (2004) 175–189.

[6] M.J.P. Brugmans, W.L. Vos, Competition between vitrification and crystallization of methanol at high pressure, J. Chem. Phys. 103 (1995) 2661–2669.

[7] J.-S. Cho, S.-H. Chun, S.-J. Lee, I.-H. Kim, D.-I. Kim, Development of cell line preservation method for research and industry producing useful metabolites by plant cell culture, Biotechnol. Bioprocess Eng. 5 (2000) 372–378.

[8] P. Clark, G.M. Fahy, A.M. Karow, Factors influencing renal cryopreservation. II. Toxic effects of three cryoprotectants in combination with three vehicle solutions in nonfrozen rabbit cortical slices, Cryobiology. 21 (1984) 274–284.

[9] S.M. Coward, C. Legallais, B. David, M. Thomas, Y. Foo, D. Mavri-Damelin, H.J. Hodgson, C. Selden, Alginate-encapsulated HepG2 cells in a fluidized bed bioreactor maintain function in human liver failure plasma, Artif. Organs. 33 (2009) 1117–1126.

[10] M.J. Dijkstra-Tiekstra, S. Hazelaar, E. Gkoumassi, M. Weggemans, J. de Wildt-Eggen, Comparison of cryopreservation bags for hematopoietic progenitor cells using a WBC-enriched product, Transfus. Apher. Sci. 52 (2015) 187–193.

[11] E. Erro, J. Bundy, I. Massie, S.-A. Chalmers, A. Gautier, S. Gerontas, M. Hoare, P. Sharratt, S. Choudhury, M. Lubowiecki, I. Llewellyn, C. Legallais, B. Fuller, H. Hodgson, C. Selden, Bioengineering the liver: scale-up and cool chain delivery of the liver cell biomass for clinical targeting in a bioartificial liver support system, Biores. Open Access. 2 (2013) 1–11.

[12] G.M. Fahy, C. daMout, L. Tsonev, B. Khirabadi, P. Mehl, H.T. Meryman, Cellular injury associated with organ cryopreservation: chemical toxicity and cooling injury, in: J.J. Lemasters, C. Oliver (Eds.), Cell Biol. Trauma, CRC Press, Boca Raton, 1995.

[13] G.M. Fahy, B. Wowk, Principles of cryopreservation by vitrification, Methods Mol. Biol. 1257 (2015) 21–82.

[14] G.M. Fahy, B. Wowk, J. Wu, J. Phan, C. Rasch, A. Chang, E. Zendejas, Cryopreservation of organs by vitrification: perspectives and recent advances, Cryobiology. 48 (2004) 157–178.

[15] J. Farrant, Mechanism of Cell Damage During Freezing and Thawing and its Prevention, Nature. 205 (1965) 1284–1287.

[16] R. Fleck, B. Fuller, Medicines from animal cell cultures, in: 2007.

[17] K.K. Fleming, A. Hubel, Cryopreservation of hematopoietic and non-hematopoietic stem cells, Transfus. Apher. Sci. 34 (2006) 309–315.

[18] X. He, E.Y.H. Park, A. Fowler, M.L. Yarmush, M. Toner, Vitrification by ultra-fast cooling at a low concentration of cryoprotectants in a quartz micro-capillary: A study using murine embryonic stem cells, Cryobiology. 56 (2008) 223–232.

[19] C.J. Hunt, Studies on cellular structure and ice location in frozen organs and tissues: The use of freeze-substitution and related techniques, Cryobiology. 21 (1984) 385–402.

[20] N.M. Jomha, A.D.H. Weiss, J. Fraser Forbes, G.K. Law, J.A.W. Elliott, L.E. McGann, Cryoprotectant agent toxicity in porcine articular chondrocytes, Cryobiology. 61 (2010) 297–302.

[21] P. Kilbride, G.J. Morris, S. Milne, B. Fuller, J. Skepper, C. Selden, A scale down process for the development of large volume cryopreservation, Cryobiology. 69 (2014) 367–375.

[22] C. Koshimoto, P. Mazur, Effects of cooling and warming rate to and from -70 degrees C, and effect of further cooling from -70 to -196 degrees C on the motility of mouse spermatozoa, Biol. Reprod. 66 (2002) 1477–1484.

[23] L.L. Kuleshova, X.W. Wang, Y.N. Wu, Y. Zhou, H. Yu, Vitrification of encapsulated hepatocytes with reduced cooling and warming rates, Cryo Letters. 25 (2004) 241–254.

[24] F. Lahnsteiner, The effect of internal and external cryoprotectants on zebrafish (Danio rerio) embryos, Theriogenology. 69 (2008) 384–396.

[25] F. Lahnsteiner, N. Mansour, T. Weismann, The cryopreservation of spermatozoa of the burbot, Lota lota (Gadidae, Teleostei), Cryobiology. 45 (2002) 195–203.

[26] A. Lawson, H. Ahmad, A. Sambanis, Cytotoxicity effects of cryoprotectants as single-component and cocktail vitrification solutions, Cryobiology. 62 (2011) 115–122.

[27] J.-H. Lee, D.-H. Jung, D.-H. Lee, J.-K. Park, S.-K. Lee, Effect of spheroid aggregation on susceptibility of primary pig hepatocytes to cryopreservation, Transplant. Proc. 44 (2012) 1015–1017.

[28] R.L. Levin, E.G. Cravalho, C.E. Huggins, Water transport in a cluster of closely packed erythrocytes at subzero temperatures, Cryobiology. 14 (1977) 549–558.

[29] R. Magalhães, B. Nugraha, S. Pervaiz, H. Yu, L.L. Kuleshova, Influence of cell culture configuration on the post-cryopreservation viability of primary rat hepatocytes, Biomaterials. 33 (2012) 829–836.

[30] R. Magalhães, X.W. Wang, S.S. Gouk, K.H. Lee, C.M. Ten, H. Yu, L.L. Kuleshova, Vitrification successfully preserves hepatocyte spheroids, Cell Transplant. 17 (2008) 813–828.

[31] I. Massie, C. Selden, H. Hodgson, B. Fuller, Cryopreservation of encapsulated liver spheroids for a bioartificial liver: reducing latent cryoinjury using an ice nucleating agent, Tissue Eng. Part C. Methods. 17 (2011) 765–774.

[32] I. Massie, C. Selden, H. Hodgson, B. Fuller, Storage temperatures for cold-chain delivery in cell therapy: a study of alginate-encapsulated liver cell spheroids stored at -80°c or -170°c for up to 1 year, Tissue Eng. Part C. Methods. 19 (2013) 189–195.

[33] I. Massie, C. Selden, H. Hodgson, B. Fuller, S. Gibbons, G.J. Morris, GMP Cryopreservation of Large Volumes of Cells for Regenerative Medicine: Active Control of the Freezing Process., Tissue Eng. Part C. Methods. 20 (2014) 1–46.

[34] J. Matheny, A.M. Karow, O. Carrier, Toxicity of dimethyl sulfoxide and magnesium

582 as a function of temperature, Eur. J. Pharmacol. 5 (1969) 209–212.
583 [35] N. Oberstein, M.K. O'Donovan, J.E. Bruemmer, J. Seidel, E.M. Carnevale, E.L.
584 Squires, Cryopreservation of equine embryos by open pulled straw, cryoloop, or
585 conventional slow cooling methods, Theriogenology. 55 (2001) 607–613.
586 [36] J. Park, Z. Fan, C.X. Deng, Effects of shear stress cultivation on cell membrane
587 disruption and intracellular calcium concentration in sonoporation of endothelial cells,
588 J. Biomech. 44 (2011) 164–169.
589 [37] D.E. Pegg, The relevance of ice crystal formation for the cryopreservation of tissues
590 and organs, Cryobiology. 60 (2010) S36–S44.
591 [38] D.E. Pegg, L. Wang, D. Vaughan, Cryopreservation of articular cartilage. Part 3: the
592 liquidus-tracking method, Cryobiology. 52 (2006) 360–368.
593 [39] D.E. Pegg, L. Wang, D. Vaughan, C.J. Hunt, Cryopreservation of articular cartilage.
594 Part 2: mechanisms of cryoinjury, Cryobiology. 52 (2006) 347–359.
595 [40] E. Puschmann, C. Selden, S. Butler, B. Fuller, Liquidus tracking: controlled rate
596 vitrification for the cryopreservation of larger volumes and tissues., Cryo Letters. 35
597 (2014) 345–355.
598 [41] A.M. Saeed, M.J. Escribá, M.A. Silvestre, F. Garcia-Ximénez, Vitrification and rapid-
599 freezing of cumulus cells from rabbits and pigs, Theriogenology. 54 (2000) 1359–
600 1371.
601 [42] S. Seki, T. Kouya, R. Tsuchiya, D.M. Valdez, B. Jin, C. Koshimoto, M. Kasai, K.
602 Edashige, Cryobiological properties of immature zebrafish oocytes assessed by their
603 ability to be fertilized and develop into hatching embryos, Cryobiology. 62 (2011) 8–
604 14.
605 [43] C. Selden, C.W. Spearman, D. Kahn, M. Miller, A. Figaji, E. Erro, J. Bundy, I. Massie,
606 S.A. Chalmers, H. Arendse, A. Gautier, P. Sharratt, B. Fuller, H. Hodgson, Evaluation

of encapsulated liver cell spheroids in a fluidised-bed bioartificial liver for treatment of ischaemic acute liver failure in pigs in a translational setting, PLoS One. 8 (2013).

[44] Y.S. Song, S. Moon, L. Hulli, S.K. Hasan, E. Kayaalp, U. Demirci, Microfluidics for cryopreservation, Lab Chip. 9 (2009) 1874–1881.

[45] G.N. Stacey, S. Dowall, Cryopreservation of primary animal cell cultures., in: Cryopreserv. Free. Protoc., 2007: pp. 271–281.

[46] C.A. Valdez, O. Abas Mazni, Y. Takahashi, S. Fujikawa, H. Kanagawa, Successful cryopreservation of mouse blastocysts using a new vitrification solution, J. Reprod. Fertil. 96 (1992) 793–802.

[47] L. Wang, D.E. Pegg, J. Lorrison, D. Vaughan, P. Rooney, Further work on the cryopreservation of articular cartilage with particular reference to the liquidus tracking (LT) method, Cryobiology. 55 (2007) 138–147.

[48] W.H. Weihe, The effect of temperature on the action of drugs, Annu. Rev. Pharmacol. 13 (1973) 409–425.

[49] B. Wowk, E. Leitl, C.M. Rasch, N. Mesbah-Karimi, S.B. Harris, G.M. Fahy, Vitrification enhancement by synthetic ice blocking agents, Cryobiology. 40 (2000) 228–236.

[50] B. Wowk, E. Leitl, C.M. Rasch, N. Mesbah-Karimi, S.B. Harris, G.M. Fahy, Vitrification enhancement by synthetic ice blocking agents, Cryobiology. 40 (2000) 228–236.

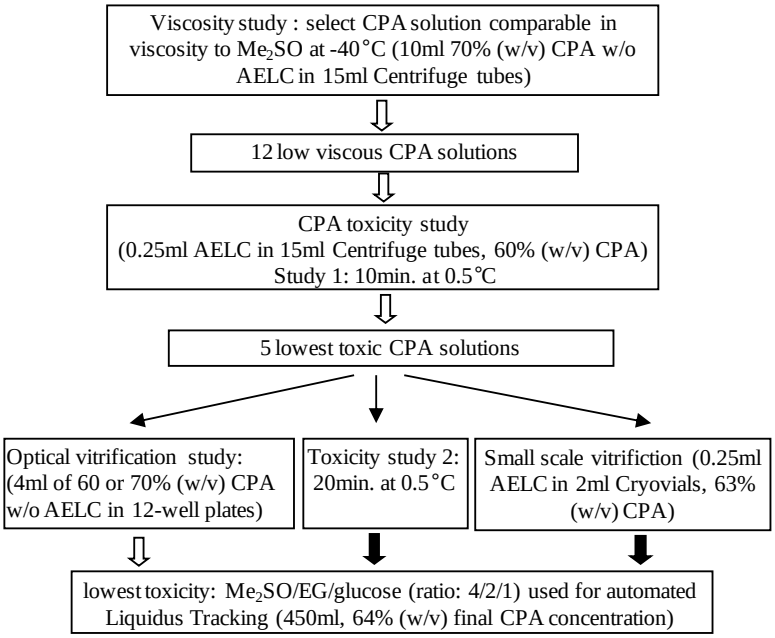

Figure 1: CPA development

Step 1: compare viscosity of combinations of Me_2SO, EG, PG, glucose (in increments of 10% (w/v)) and methanol (10% (w/v)) to Me_2SO alone at -40°C. Select combinations with similar viscosity to Me_2SO. Step 2: test toxicity of low viscous CPA solutions on AELC (10 minutes at 0.5°C). Step 3: repeat step 3 for 5 lowest toxic CPA solutions for 20 minutes. Step 4: test 5 lowest toxic CPA solutions in a standard small scale vitrification process. Step 6: visual observation of vitrification properties of 5 low toxic CPA solution. Step 1-6: Incubation time and volumes were optimized for each test.

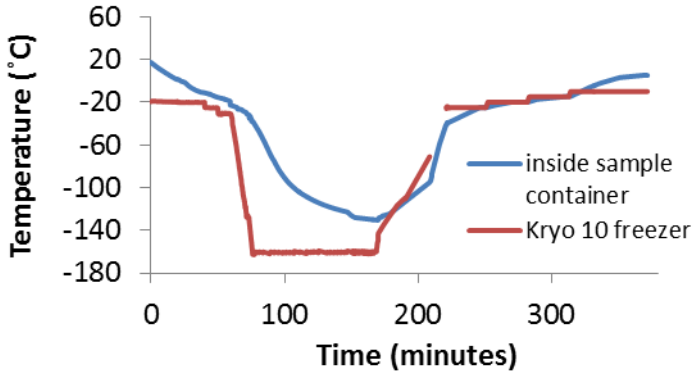

Figure 2: The LT cooling and warming profile

Temperature profile of the LT sample and the freezer were assessed by thermocouples being placed inside the sample (blue line), and inside the freezer chamber (red line). When the sample reached a temperature of -95˚C during warming, the sample container was placed outside the freezer at room temperature (indicated by the interrupted red line at 200 minutes when the chamber was opened) for fast initial warming to achieve a core sample temperature of -40˚C. The freezer chamber temperature was also set at -40˚C, and the sample was returned to the chamber for the reverse LT process. To increase the sample temperature further, the freezer temperature was set manually from initially -25˚C to -20˚C then -15˚C and finally -10˚C, to keep the sample temperature above its liquidus curve and prevent freezing.

.

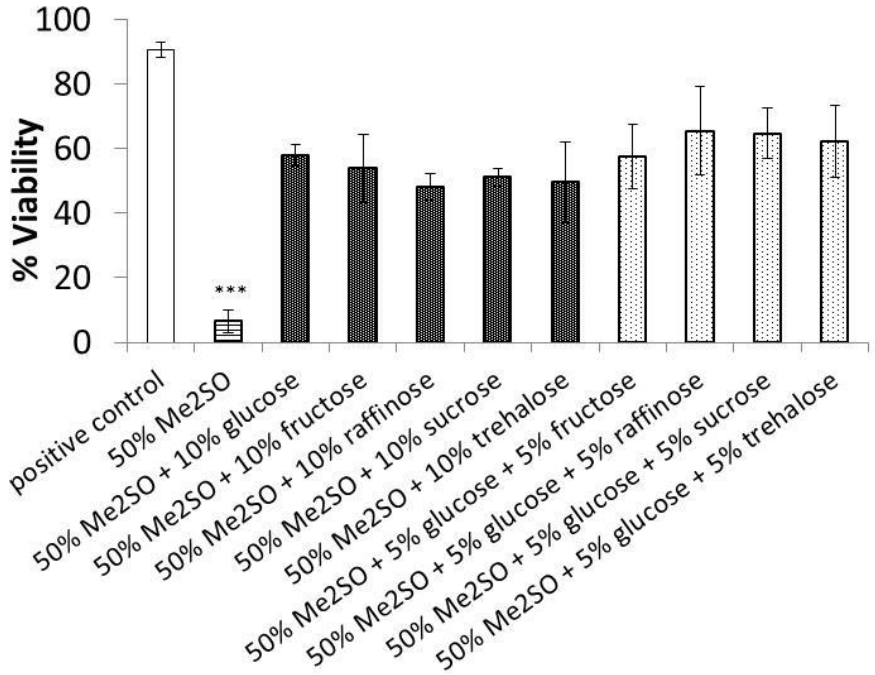

Figure 3: Sugars and sugar combination as non-penetrating CPA — effect in cell viability

AELC (0.25ml) were incubated in 50% (w/v) Me_2SO (white) or 50% (w/v) Me_2SO plus 10% (w/v) sugar, either of one single sugar (grey) or two different sugars (light grey). AELC were incubated for 10 minutes at 0.5˚C, using a step-wise CPA addition and reduction procedure. AELC were cultured for 24 hours in complete media at 37˚C before measuring viability by FDA/PI staining. Data were n=5 +/- SD. Viability obtained with 50% (w/v) Me_2SO was significantly lower than with solutions containing sugar, ***p<0.001.

669

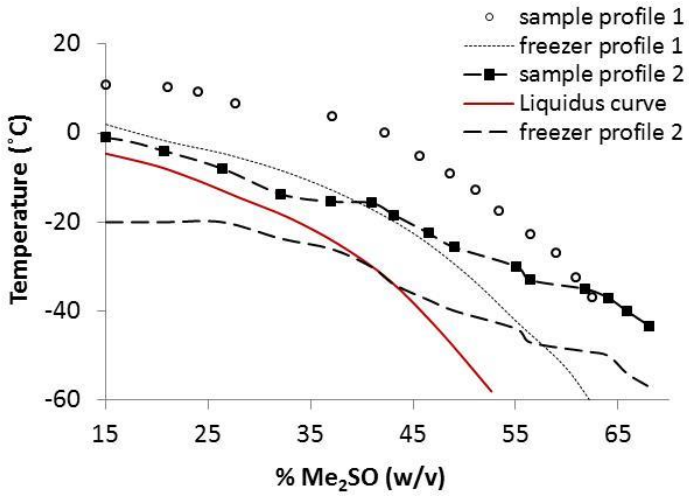

670

671 **Figure 4: Freezer and sample cooling profile relative to the liquidus curve**

672 **Solutions with CPA concentrations below the liquidus curve (red) freeze, while those above remain liquid.**
673 **Liquidus Tracking: by keeping the sample temperature and CPA concentration just above the liquidus**
674 **curve, CPA toxicity was reduced and ice nucleation avoided. Freezer cooling profile 1 resulted in a**
675 **discrepancy of ˜15˚C of the obtained sample profile (profile 1) to the expected profile (not shown) and was**
676 **approximately 20˚C higher than the liquidus curve. To increase the sample cooling rate (sample profile 2)**
677 **the freezer temperature (freezer profile 2) was initially set to -20˚C below the liquids curve.**

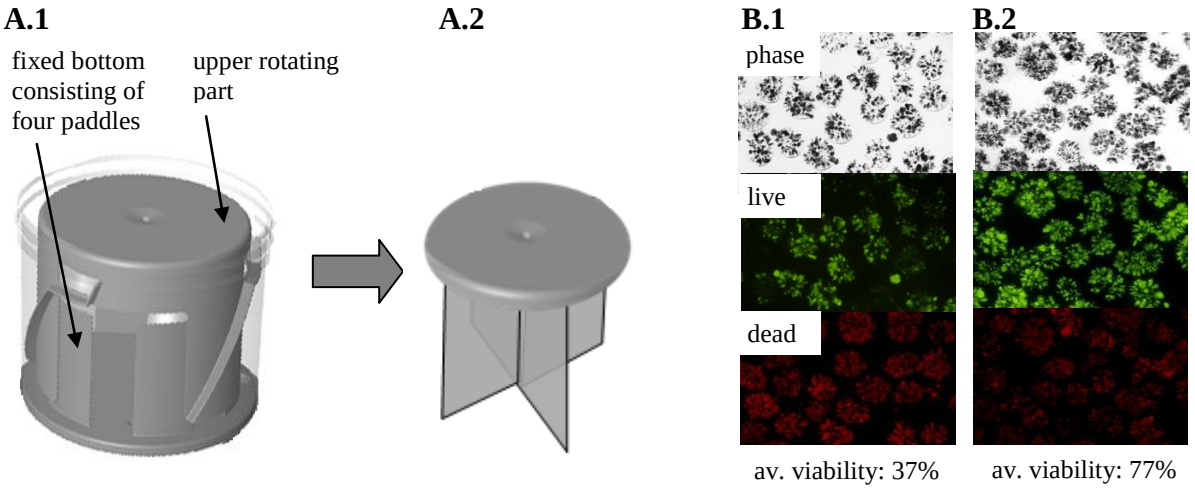

Figure 5: Planer stirrer versus propeller stirrer

A1: Planer stirrer — the paddles of the upper part move between the sample carrier wall and the paddles of the bottom part - possibly creating strong differences in mixing behaviour and shear forces between the sample carrier centre and on the outside. A2: Propeller stirrer — used for more homogenous mixing. B1: AELC viability after using the Planer stirrer. B2: Propeller stirrer — viability was significantly increased and bead to bead viability variation was reduced. The figure shows phase images, and images of live (green, stained with FDA) and dead (red, stained with PI) cells.

Note: Figure 5- please print in color

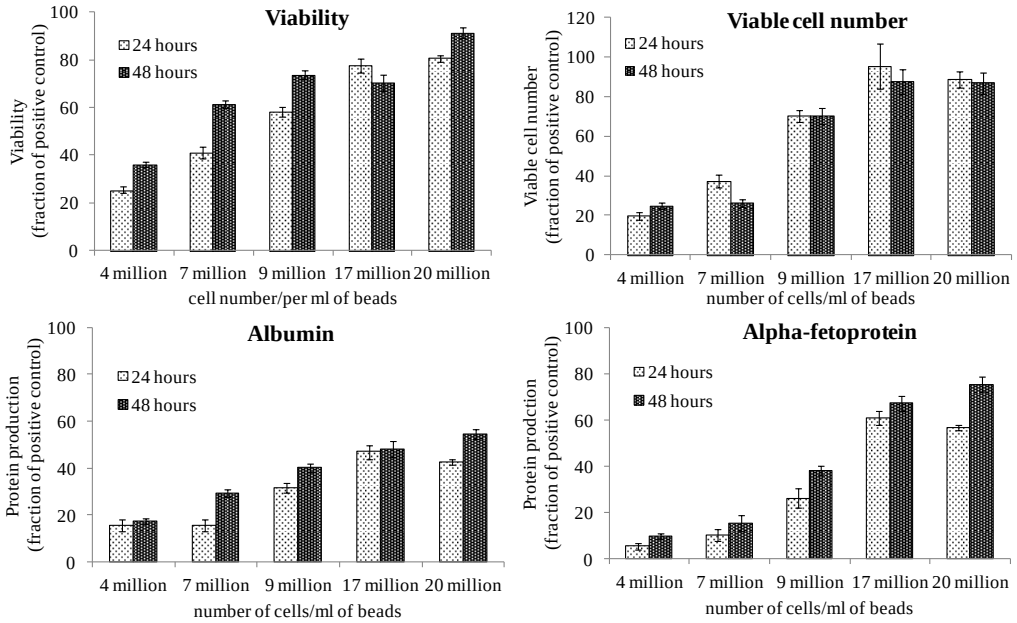

Figure 6: Impact of low and high cell densities on cell recovery

The higher the cell density was before the LT process (4, 7, 9, 17, 20 million cells/ml of beads), the higher was the post-warming viability, viable cell number, albumin and alpha-fetoprotein synthesis. For each cell density one LT run was performed. Viability, cell number and protein production were measured in 5 replicates for each sample, and shown as means +/- SE . 130ml of beads in 450ml CPA were used.